

## 2,3-Diphenylbutadiene and Donor–Acceptor Functionalized Derivatives: Exploring the Competition between Conjugation Paths in Branched $\pi$ -Systems

Peter A. Limacher and Hans Peter Lüthi\*

Laboratory of Physical Chemistry, Swiss Federal Institute of Technology, Wolfgang-Pauli-Str. 10, 8093 Zürich, Switzerland

Received: November 30, 2007; In Final Form: January 18, 2008

2,3-Diphenylbutadiene and its donor–acceptor functionalized derivatives represent branched  $\pi$  systems consisting of three overlapping linearly conjugated units, namely a 1,3-butadiene and two phenylethene subsystems. The evaluation of  $\pi$  conjugation using a scheme based on the natural bond orbital analysis shows that the details of the structure of these compounds is governed by electron delocalization. The potential energy surface of 2,3-diphenylbutadiene shows two minima, each one representing a distinct combination of conjugation patterns. These minima are shown to be connected by a low-energy path with transition structures that have one conjugation path fully activated, while conjugation is completely disrupted along the other path. We will show that, in response to donor–acceptor functionalization, the 2,3-diphenylbutadiene backbone will switch to other conformations, which come along with substantial changes in the electronic structure.

### Introduction

2,3-Diphenylbutadiene (**1**) represents a generic branched  $\pi$  system consisting of three overlapping linearly through-conjugated units, namely a 1,3-butadiene and two phenylethene subsystems (here also referred to as styrene subsystems). Furthermore, the two phenyl rings are coupled via cross-conjugation over the butadiene backbone. Steric strain due to overlapping hydrogen atoms in the *s-trans*, and, even more so in the *s-cis* geometry prevents the molecule from being planar. This will result in a loss of  $\pi$  delocalization energy, and the details of the structure of these compounds will be greatly influenced by the competition between conjugation pathways. The 2,3-diphenylbutadiene framework thus renders itself nicely for the study of through- and cross-coupled donor–acceptor (D–A) systems. Furthermore, derivatives of 2,3-diphenylbutadiene may show potential as functional materials. Obviously, the properties of these compounds strongly depend on the type of functional groups present and on the pathway connecting them.

In the course of their studies of branched  $\pi$  conjugated systems, van Walree and co-workers recently reported on the molecular and electronic structure of 2,3-diphenylbutadiene **1**.<sup>1,2</sup> In earlier work, the same authors reported on evidence for charge transfer (CT) in 2-(4-cyanophenyl)-3-(4-*N,N*-dimethylaminophenyl)-butadiene (**2**) along the bifurcated (i.e. cross-coupled)  $\pi$  system of butadiene, indicating that these compounds may be used in the development of materials with multiple conduction channels.<sup>3</sup> Diederich and co-workers have synthesized and characterized an extensive series of donor-substituted tetracyano-butadienes, some of which show strong intramolecular CT despite the nonplanarity of the compounds.<sup>4,5</sup> Some of these, such as 2,3-bis(4-*N,N*-dimethylaminophenyl)-1,1,4,4-tetracyano-butadiene, (**3**), also show unusual redox properties (highly charged anions with very narrow reduction potential ranges).

Since the molecule is prevented from having a planar structure, which would be optimal from a  $\pi$  conjugation perspective, competition between the various conjugation paths is induced, and as long as van der Waals interactions between the phenyl rings play no major role, the resulting molecular structure will represent a compromise between styrene- and butadiene-type through-conjugation. The cross-conjugated pathways usually play a much less important role. Depending on the degree of preservation of these conjugation paths, **1** and its functionalized derivatives will resemble either a substituted butadiene, an  $\alpha,\alpha$ -coupled bistyrene or a mixture thereof. Accordingly, the crystal structure of **1** reported by van Walree is best described as a system which retains much of the styrene conjugation but still shows some butadiene conjugation.<sup>1</sup>

Since the structure and properties of these compounds are governed by relatively weak interactions allowing for several minimum energy structures, the potential energy surface (PES) of these compounds may be rather complex. In this work we first investigate  $\pi$  conjugation as a function of the molecular structure of unsubstituted 2,3-diphenylbutadiene. We will then focus on the structure and electronic properties of the cross- and trans-coupled D–A systems **2** and **3**.

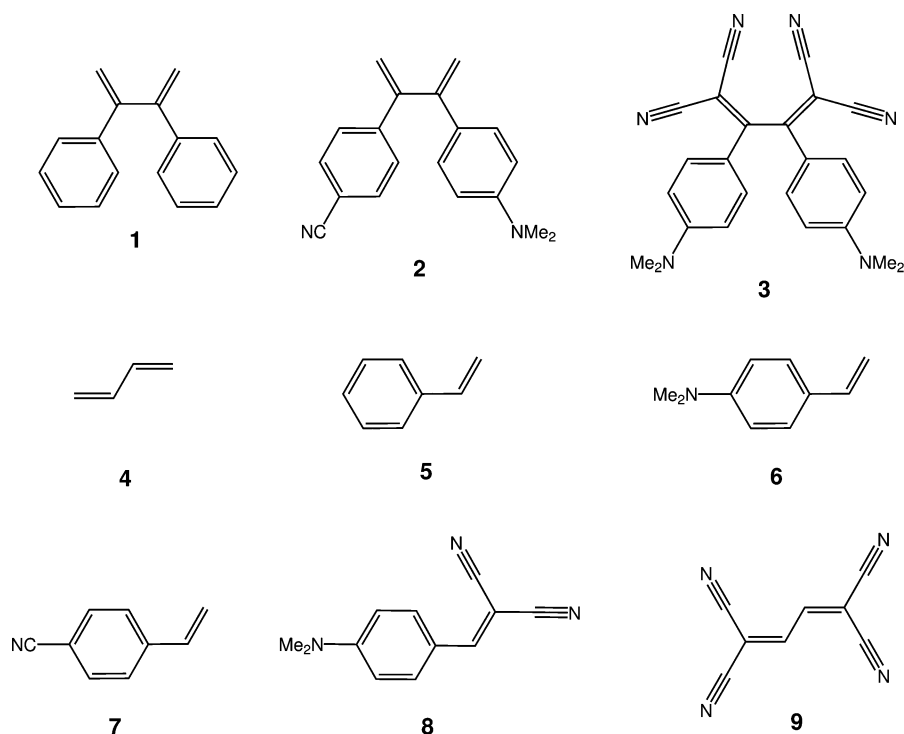
Even though it is not a physical observable, the quantitative evaluation of electron delocalization has obtained considerable attention,<sup>6,7</sup> as it helped to explain complex features by means of a popular and widely used concept.<sup>8–10</sup> In this work we will apply a method for the evaluation of the delocalization energy which is based on the natural bond orbital (NBO) analysis<sup>11</sup> and which has been successfully applied in earlier studies of through- and cross-conjugated two-dimensional  $\pi$  systems.<sup>12–14</sup>

### Computational Methods

**Molecular and Electronic Structure Calculation.** All calculations were performed at the B3LYP/6-311G\*\* level using the program Gaussian 03.<sup>15</sup> Structures **1a**, **1b**, **2a**, **2b**, **3**, **3<sup>2-</sup>**, **4**, **5**, **6**, **7**, **8**, **8<sup>-</sup>**, **9**, **9<sup>-</sup>**, and **9<sup>2-</sup>** were verified to be minima by performing frequency calculations. The transition states **1c**

\* To whom correspondence should be addressed. E-mail: luethi@phys.chem.ethz.ch.

## SCHEME 1: All Compounds Considered in This Study



and **1d** were located by means of the synchronous transit-guided quasi-Newton (STQN) method implemented in Gaussian 03.

Additionally, structures **1a–1d** were optimized at the MP2/6-311++G\*\* level of theory, mainly in order to investigate the importance of the van der Waals interactions between the phenyl rings as observed in the literature.<sup>16</sup> It will be shown below that the MP2 computations do not lead to a significant change neither in the relative energy of the stationary points nor in the corresponding molecular structures. We also are in good agreement with the calculations on **1a** and **1b** reported by van Walree.<sup>2</sup>

Another crucial point is the influence of diffuse basis functions on the molecular structure, especially of the anions. To ensure that such effects are not present here, the structures of **3** and **3<sup>2-</sup>** were reoptimized at the B3LYP/6-311++G\*\* level. The final molecular structures show no significant differences in bond lengths or torsion angles neither in the neutral nor in the charged species. Therefore, the method of choice for this study is B3LYP/6-311G\*\*.

The total energy of the global minimum **1a** computed at the B3LYP/6-311G\*\* level is  $-618.250003$  a.u. and at the MP2/6-311++G\*\* level  $-616.368218$  a.u. All open shell calculations of the radical anions were performed in a spin unrestricted scheme.

**Analysis of Conjugation Properties.** The investigation of quantities related to  $\pi$  conjugation, such as delocalization energies, orbital occupations and orbital interactions was performed on the basis of the NBO scheme introduced by Weinhold.<sup>11</sup> It has been shown that the NBO analysis can be used to study electron delocalization in  $\pi$ -conjugated systems, even at the level of the individual paths.<sup>13,14</sup> The procedure is not restricted to the analysis of (vertical)  $\pi$  conjugation, but can be applied also to study of in-plane  $\pi$  and  $\sigma$  conjugation.<sup>12</sup>

The delocalization energies reported here were obtained by deletion of the weakly occupied  $\pi^*$  orbitals that are part of the conjugation path under consideration from the Fock matrix in

NBO basis. In this model, the difference between the total energy computed in full and in reduced NBO space is a measure of the delocalization energy.

In this work we will also use second order orbital interaction energies between neighboring orbitals in a given path as expressed by the equation

$$E_{i \rightarrow j} = n_i \frac{F(i,j)^2}{\epsilon_i - \epsilon_j}$$

where  $i$  and  $j$  point at a pair of interacting donor and acceptor NBOs.  $\epsilon_i$  and  $\epsilon_j$  are the respective orbital energies (i.e., the diagonal elements of the Fock matrix),  $F(i,j)$  is the corresponding off-diagonal element of the Fock matrix, and  $n_i$  is the donor orbital occupation number.

The localization of the electronic charge into one- and two-center orbitals in the NBO method is dependent on the underlying Lewis structure. In a charged species, the optimal (dominant) Lewis structure may be different from the one of the neutral molecule. This makes the comparison of NBOs across the charged and uncharged species difficult. Also, the singly charged anions considered here are open shell systems, which may have different optimal Lewis structures for the  $\alpha$  and the  $\beta$  spin components of the electron density.

In the present study we will encounter situations where the optimal Lewis structure will indeed change. Performing the NBO analysis on different sets of Lewis structures does lead to different numerical results, but, in the present case, does not affect the conclusions to be taken. Using nonoptimal Lewis structures will have the consequence that the orbital interactions will increase. In addition, self-interaction of a  $\pi$  orbital with its own  $\pi^*$  orbital is observed, if a double bond is assigned where a single bond would be the more appropriate description. This is not an artifact of the NBO method but an intrinsic effect of the rearrangement of the electronic structure upon reduction.

The orbital occupations however, being based on natural atomic orbitals (NAOs), are not nearly as strongly affected by the choice of the Lewis structure.

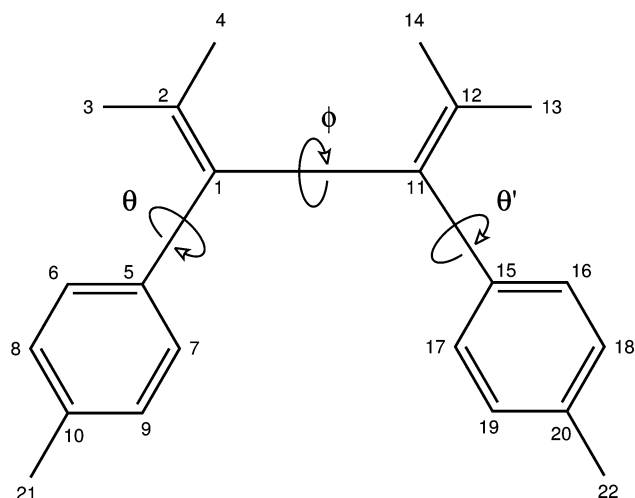


**Figure 1.** Atom labels and the three dihedral angles  $\phi$ ,  $\theta$  and  $\theta'$  which are defined by the quartets of atoms  $\phi$  (C(2)–C(1)–C(11)–C(12)),  $\theta$  (C(2)–C(1)–C(5)–C(6)), and  $\theta'$  (C(12)–C(11)–C(15)–C(16)). In symmetric molecules  $\theta$  and  $\theta'$  are identical.

All NBO calculations were performed with the package NBO version 3.1 included in Gaussian 03.

## Results and Discussion

**Molecular and Electronic Structures of 2,3-Diphenylbutadiene.** The structure of compound **1** is best described by the three dihedral angles  $\phi$ ,  $\theta$ , and  $\theta'$  as defined in Figure 1. If  $C_2$  symmetry is retained, the angles  $\theta$  and  $\theta'$  will be identical. Rotation about  $\phi$  will disrupt  $\pi$  conjugation of the butadiene fragment, whereas rotation about  $\theta$  and  $\theta'$  will disrupt  $\pi$  conjugation in the styrene subunits.

A scan of the PES of 2,3-diphenylbutadiene as a function of the angles  $\phi$  and  $\theta$  is presented in Figure 2a. Figure 2b is a periodic replica of Figure 2a, offering a more extended view of the PES. The PES shows two minima, denoted **1a** and **1b**, that are very close in energy (0.23 kcal/mol difference). The energy maxima in the four corners of Figure 2a represent planar structures suffering from steric strain.

In Figure 2b we can follow the diagonal valley that interconnects the global minimum **1a** and the local minimum **1b** via a transition state **1c**, which is 3.01 kcal/mol above the global minimum. A second transition state, **1d**, representing a barrier of 1.03 kcal/mol, connects **1b** with its mirror image **1b'**. The transition state connecting **1a** directly with its mirror image **1a'** lies much higher in energy ( $\sim 6$  kcal/mol), but is of less importance, as a lower energy path along the valley is available (as marked in Figure 2b).

In the MP2 calculations, the global minimum **1a** is stabilized by 1.47 kcal/mol, whereas transition structure **1c** is destabilized by 0.85 kcal/mol. The energy of the two other stationary points is not significantly affected. The barrier between **1a** and **1b** is predicted to amount to 5.33 rather than 3.01 kcal/mol, whereas the barrier connecting **1b** with **1b'** changes by 0.07 kcal/mol only. For all four conformations of **1**, the MP2 bond lengths systematically differ by about  $-0.007$  Å for single bonds, and  $+0.012$  Å for double bonds relative to the density functional (DFT) calculations. The relative bond lengths as well as the ordering of the energy of the minima and transition states remain unchanged. Most importantly, torsion angles were found to deviate by no more than  $7^\circ$  from the values obtained from DFT calculations. This indicates that van der Waals interactions play only a minor role in the molecules considered in this study.

The discussion presented below is therefore based on the results obtained from the DFT calculations.

Figure 3 gives a schematic overview of the structures **1a** to **1d**. The minima **1a** and **1b** are distorted s-cis and s-trans butadienes, whereas for transition states **1c** and **1d** we find planar fragments with undisturbed conjugation paths. The relevant structural parameters of these four stationary points are listed in Table 1. They are compared with the crystal structure reported by van Walree.<sup>1</sup>

The conformation of **1a** with angles  $\phi = 55.2^\circ$  and  $\theta = 34.5^\circ$  is best described as a bistyrene-like structure with some butadiene conjugation retained, whereas the conformation of **1b**, with angles  $\phi = 154.6^\circ$  and  $\theta = 130.8^\circ$ , more closely resembles a butadiene-like structure with some styrene conjugation retained. Transition state **1c**, on the other hand, has a nearly perfect bistyrene structure ( $\theta = 170.7^\circ$ ) with an almost fully twisted butadiene backbone ( $\phi = 91.1^\circ$ ). The transition state **1d** takes a perfect s-trans butadiene structure with the phenyl rings perpendicular to the butadiene plane ( $C_{2h}$  symmetry). The higher energy transition state (not listed for the reason quoted above) reflect a configuration with a perfect s-cis butadiene structure, but with the phenyl rings  $90^\circ$  distorted out of the conjugation plane ( $C_{2v}$  symmetry).

The experimental structure strongly resembles the global minimum **1a**.<sup>1</sup> The angle  $\phi$  is the same within  $1^\circ$ . Both angles  $\theta$  are smaller by about  $17^\circ$ . It is reasonable to assume that the smaller angles are due to crystal packing effects, which end up further enhancing conjugation within the styrene subunits at the expense of steric strain.

Inspection of Table 1 also shows that the computed bond lengths of **1a** and those determined experimentally are the same within a small margin (less than 0.01 Å for the C(1)–C(11) and C(1)–C(5) single bonds; about 0.01 Å for the C(1)–C(2) double bonds). A short C(1)–C(11) single bond indicates good butadiene conjugation as found in **1b** and especially in **1d**. In contrast, a short C(1)–C(5) single bond points at good conjugation in the styrene subunit, as observed for **1a** and **1c**. The C(1)–C(2) length is somewhat indifferent, as both (styrene and butadiene) conjugation paths tend to elongate that particular double bond. The quinoid character  $\delta r$  is strongest for styrene-like conformations (**1a** and **1c**).

The molecular structure of 2,3-diphenylbutadiene evidently follows a simple pattern: while the minimum energy structures represent conformations with a sophisticated balance between styrene and butadiene conjugation, the transition structures represent conformations with one conjugation path fully turned on, and the other one completely switched off, an observation shared with the study of van Walree.<sup>2</sup>

These findings can be further illustrated by means of the analysis of the electronic structure of the compound. Figure 2c shows the calculated delocalization energy for the same geometries as in Figure 2a. The delocalization energy is largest ( $\sim 315$  kcal/mol) in the nearly planar region ( $\phi$  and  $\theta$  are close to  $0^\circ$  or  $180^\circ$ ), while the smallest delocalization energy ( $\sim 280$  kcal/mol) is found in the region where all  $\pi$  systems are orthogonal to each other ( $\phi$  and  $\theta$  around  $90^\circ$ ). The delocalization energy at this point essentially stems from the aromatic phenyl rings.

The energetic properties (total energies, delocalization energies, and orbital interaction energies) of the stationary points **1a–d** are shown in Table 2 and, whenever possible, are compared with the corresponding values of isolated s-trans butadiene **4** and styrene **5**.

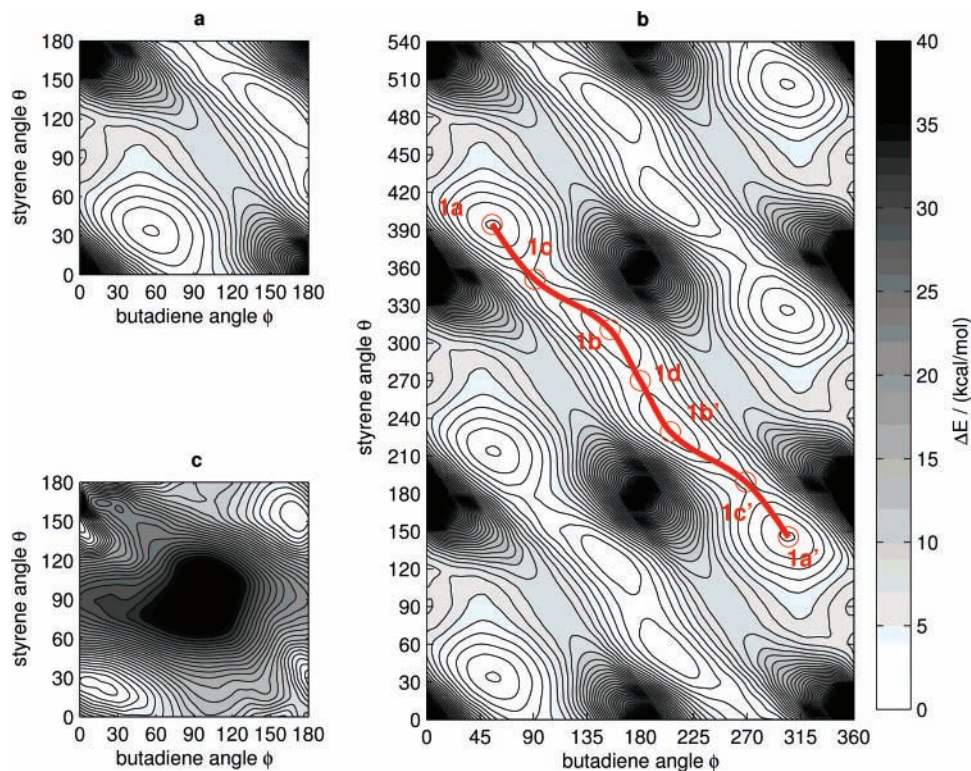


**Figure 2.** Potential energy surface of **1**. Panel a shows the total energy as a function of the angles  $\phi$  and  $\theta$  (gridsize  $10^\circ$ ) with relaxation of all other geometry parameters. The spacing between two contours corresponds to 1 kcal/mol difference in energy, and is taken relative to the global minimum. Two minima can be found. Panel b offers an extended view of the scanned region. The path highlighted in this panel connects the global minimum **1a** with the local minimum **1b** and their corresponding mirror images **1a'** and **1b'**. Two different transition states can be found along this path (**1c** and **1d**). **1c'** is the transition state on the path **1a'**–**1b'** and is the mirror image of **1c**. Panel c shows the delocalization energy calculated by deletion of all the eight antibonding  $\pi^*$  orbitals of **1**. The regions with highest delocalization are the nearly planar geometries which, however, are not accessible due to steric strain.

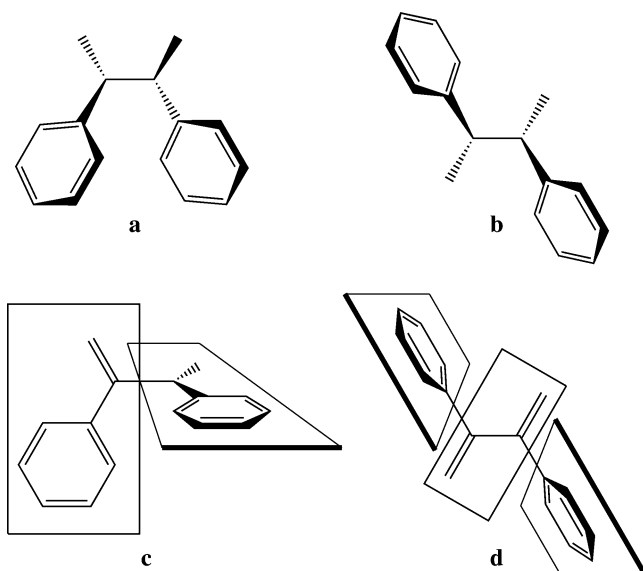


**Figure 3.** Schematic representation of the four stationary points of **1**. Similar structures are also observed for the substituted compounds **2** and **3**.

The transition from **1a** to **1b** through **1c** includes an s-cis  $\rightarrow$  s-trans inversion and therefore corresponds to the rotational barrier in butadiene **4**. Similarly, the transition from **1b** to **1b'** through **1d** corresponds to the rotational barrier in styrene **5**. Inspection of Table 2 shows that the barrier height in both cases is about three times smaller than in the reference systems (**4** and **5**), as delocalization in the styrene unit can compensate for the missing butadiene interaction in conformation **1c**, and vice

**TABLE 1: Selected Geometry Parameters<sup>a</sup> of **1** (in Å or deg)**

|                   | C(1)–C(11) | C(1)–C(5) | C(1)–C(2) | $\delta r^b$ | $\phi$  | $\theta$ |
|-------------------|------------|-----------|-----------|--------------|---------|----------|
| <b>1a</b>         | 1.4970     | 1.4894    | 1.3411    | 0.0067       | 55.2    | 34.5     |
| <b>1b</b>         | 1.4905     | 1.4936    | 1.3431    | 0.0054       | 154.6   | 130.8    |
| <b>1c</b>         | 1.5097     | 1.4898    | 1.3392    | 0.0083       | 91.1    | 170.7    |
| <b>1d</b>         | 1.4829     | 1.4992    | 1.3414    | 0.0030       | 180.0   | 90.0     |
| lit. <sup>c</sup> | 1.492(2)   | 1.491(2)  | 1.329(3)  | 0.003(3)     | 55.6(2) | 17.0(3)  |
|                   |            | 1.486(2)  | 1.335(3)  | 0.009(3)     |         | 19.3(3)  |

<sup>a</sup> For atom numbering and definition of the bond angles see Figure 1. <sup>b</sup>  $\delta r$  is the quinoid character of the phenyl rings.<sup>18</sup> A value of  $\delta r = 0$  Å means that there is no difference between bond lengths; values around  $\delta r = 0.1$  Å are found in fully quinoid systems. <sup>c</sup> The experimental structure shows no  $C_2$  symmetry.<sup>1</sup> The torsion angles are adapted to our definitions.

versa in **1d**. As expected, **1a** shows the highest overall delocalization energy. The transition state **1d** shows the least delocalization energy, but is still energetically more stable than the apparently more conjugated transition state **1c**. This is because the phenyl rings in **1d** are in a position where they have the least possible steric hindrance, which compensates the lack of conjugation.

The conclusions drawn on the structures of **1a** to **1d** are nicely illustrated by the orbital interaction energies (Table 2). One finds that the transition state **1c** has an almost fully conjugated styrene path. In comparison with pure styrene **5**, the difference in orbital interaction energy between the double bond and the adjacent phenyl group is very small. The interaction energy between the double bonds, on the other hand, is close to zero. The opposite is true for **1d**, where styrene conjugation is switched off, but the interaction between the vinyl groups is nearly as high as in planar s-trans butadiene. The minima **1a** and **1b** show orbital

TABLE 2: Energies of Different Conformations of **1** (in kcal/mol)

|           | total energies <sup>a</sup> |                  | delocalization energies <sup>b</sup> |                                  |                                 | orbital interaction energies <sup>c</sup>       |   |   |
|-----------|-----------------------------|------------------|--------------------------------------|----------------------------------|---------------------------------|---|---|---|
|           | $E_{\text{rel}}^d$          | $E_{\text{inv}}$ | $E_{\text{del}}^{\pi}(8)$            | $E_{\text{del}}^{\text{Sty}}(4)$ | $E_{\text{del}}^{\text{Bu}}(2)$ | $\pi_{\text{Ph}} \rightarrow \pi_{\text{Ph}}^*$ | $\pi_{\text{Ph}} \rightarrow \pi_{\text{Ph}}^*$ | $\pi_{\text{Ph}} \rightarrow \pi_{\text{Ph}}^*$ |
| <b>1a</b> | 0.00                        | 3.01             | 307.61                               | 153.30                           | 33.07                           | 7.65  | 9.43  | 4.65  |
| <b>1b</b> | 0.23                        | 1.06             | 306.65                               | 152.71                           | 34.39                           | 5.41  | 5.77  | 11.70   |
| <b>1c</b> | 3.01                        |                  | 307.24                               | 153.70                           | 32.44                           | 11.26   | 13.76   | 0.09  |
| <b>1d</b> | 1.29                        |                  | 301.05                               | 151.32                           | 31.88                           | 0.06  | 0.03  | 14.65   |
| <b>4</b>  |                             | 7.11             |                                      |                                  | 24.84                           |   |   | 15.08   |
| <b>5</b>  |                             | 3.85             |                                      | 150.53                           |                                 | 11.33   | 14.80   |   |

<sup>a</sup>  $E_{\text{rel}}^d$  is the total SCF energy relative to the global minimum **1a**.  $E_{\text{inv}}$  is the energy barrier that separates **1a** and **1b** from their mirror image **1a'** and **1b'**, respectively. These energies can be related to the rotational barriers in **4** and **5**. <sup>b</sup> The delocalization energy computed by deletion of the antibonding  $\pi^*$  orbitals involved in the path under consideration. The number of orbitals deleted is given in parentheses.  $E_{\text{del}}^{\pi}$  corresponds to the deletion of all  $\pi^*$  orbitals of **1**, whereas  $E_{\text{del}}^{\text{Sty}}$  stands for the deletion of the  $\pi^*$  orbitals for one styrene fragment only.  $E_{\text{del}}^{\text{Bu}}$  is the deletion energy of the two vinylic  $\pi^*$  orbitals of the butadiene backbone. <sup>c</sup> The interaction energy between orbitals as calculated by second-order perturbation theory. Tabulated are the donor interaction of the vinyl  $\pi$  orbital with the three  $\pi^*$  orbitals of the phenyl ring ( $\pi_{\text{Ph}} \rightarrow \pi_{\text{Ph}}^*$ ), the corresponding back-donation interaction ( $\pi_{\text{Ph}} \rightarrow \pi_{\text{Ph}}^*$ ), and the interaction between the two butadiene double bonds with each other ( $\pi_{\text{Ph}} \rightarrow \pi_{\text{Ph}}^*$ ). <sup>d</sup> At the MP2/6-311++G\*\* level, the corresponding values are 0.00, 1.70, 5.33, and 2.80, respectively. Van Walree reports a relative energy difference of 1.08 kcal/mol between **1a** and **1b**.<sup>2</sup>

TABLE 3: Selected Geometry Parameters of **2** (in Å or deg) of the Donor (D) and Acceptor Fragments (A) and Comparison with **6** and **7**

| D         | C(1)–C(11)  | C(1)–C(5)   | C(1)–C(2)   | $\delta r$  | C(10)–N(21) | $\phi$    | $\theta$ |
|-----------|-------------|-------------|-------------|-------------|-------------|-----------|----------|
| <b>2a</b> | 1.4980      | 1.4831      | 1.3429      | 0.0214      | 1.3841      | 55.8      | 31.5     |
| <b>2b</b> | 1.4927      | 1.4877      | 1.3448      | 0.0202      | 1.3803      | 151.6     | 133.7    |
| <b>2c</b> | 1.5095      | 1.4830      | 1.3415      | 0.0233      | 1.3827      | 98.4      | 175.1    |
| <b>2d</b> | 1.4839      | 1.4972      | 1.3420      | 0.0161      | 1.3822      | 180.0     | 90.0     |
| <b>6</b>  |             | 1.4664      | 1.3372      | 0.0221      | 1.3864      |           | 1.2      |
| A         | C(11)–C(15) | C(11)–C(12) | $\delta r'$ | C(20)–C(22) | C(22)–N(24) | $\theta'$ |          |
| <b>2a</b> | 1.4885      | 1.3410      | 0.0161      | 1.4298      | 1.1556      | 33.4      |          |
| <b>2b</b> | 1.4920      | 1.3428      | 0.0148      | 1.4301      | 1.1555      | 130.3     |          |
| <b>2c</b> | 1.4863      | 1.3388      | 0.0173      | 1.4294      | 1.1557      | 154.3     |          |
| <b>2d</b> | 1.4982      | 1.3410      | 0.0120      | 1.4307      | 1.1554      | 90.0      |          |
| <b>7</b>  | 1.4702      | 1.3353      | 0.0179      | 1.4294      | 1.1556      | 0.0       |          |

interactions along both paths but with a clear emphasis either on styrene (**1a**) or on butadiene conjugation (**1b**).

**Donor–Acceptor Substituted 2,3-Diphenylbutadienes.** Replacement of the phenyl groups in **1** by a *p*-*N,N*-dimethylanilino (DMA) and a *p*-cyanophenyl group leads to a cross-coupled D–A system **2**. Now that the  $C_2$  symmetry is lost, different properties are observable for the donor (D) and acceptor (A) fragment of the molecule.

The geometry optimization of **2** leads to the same pattern observed for the unsubstituted compound **1**: we find two minima close in energy (**2a** and **2b**) that are separated by two transition states (**2c** and **2d**), again representing structures that have one conjugation path fully switched on, and the other one switched off. The sequence of energies in the four different structures is the same as in **1**. This means that the minimum with the more pronounced styrene conjugation (**2a**) is again lowest in energy.

The most important structural parameters are listed in Table 3, where they are compared with the isolated donor and acceptor fragments **6** and **7**. The main structural difference relative to **1** is in the enhanced quinoid character  $\delta r$  of the phenyl rings. However, this trend can already be observed in the isolated fragments **6** and **7** and is even more pronounced in these nonstrained systems.

Based on their investigation of the absorption and fluorescence spectra of **2**, van Walree and co-workers concluded that there is evidence for D–A interaction between the two functional groups, despite the presumably much less efficient cross-conjugation path with its two branching points. The comparison of the molecular structure of **1** and **2** suggests only a small difference in their electronic structure. However, the NBO population analysis shows a weak flow of charge from the (D)

fragment to the (A) fragment, which is most pronounced in structure **2b** where 0.13  $\pi$  electrons are transferred, which in this structure is still in place.

In compound **3**, where the donors and acceptors are trans rather than cross-coupled, the D–A interactions may now be strong enough to overturn the structure of the compound. However, relative to **1** and **2** the cyano groups of **3** introduce extra steric strain. The computations show only one minimum on the energy surface spanned by  $\phi$  and  $\theta$ . It is very similar to transition structure **1c** which exhibits the most pronounced styrene conjugation (Table 4). This is clearly visible from the change in bond lengths (high quinoid character of the aromatic rings along with shorter single bonds C(1)–C(5) and C(10)–N(21), plus longer double bonds). Obviously this conjugation path is so efficient that the styrene fragment becomes almost planar ( $\theta$  deviates only 25° from planarity), despite the repulsive interaction of the cyano groups with a proton of the neighboring phenyl ring. As in **1c** or **2c**, the C(1)–C(11) bond is very long with the torsion angle  $\phi$  not far from orthogonality. Furthermore, the comparison of **3** and the isolated fragment **8** shows only little difference in bond lengths.

The NBO analysis shown in Table 5, indicates that there is only marginal electronic communication between the styrenic  $\pi$  systems over the butadiene bridge: the orbital interaction along the butadiene path in **3** is vastly absent, unlike in the planar reference system **9**. On the other hand, the comparison of orbital interaction energies shows very similar values for **3** and **8**. This confirms that **3** should be viewed as two isolated styrene moieties, i.e., an  $\alpha,\alpha$ -coupled bistyryl, rather than a donor-substituted tetracyanobutadiene.

**Anions of Donor–Acceptor Substituted 2,3-Diphenylbutadienes.** The electron affinities listed in Table 5 show that

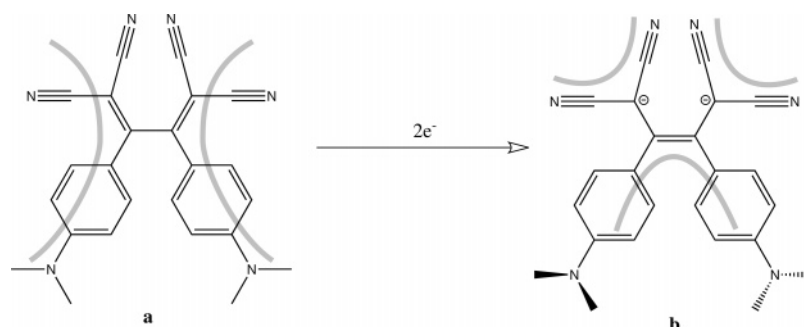
**TABLE 4: Selected Geometry Parameters of 3, 8, and 9 and Their Respective Anions (in Å or deg)**

|                       | C(1)–C(11) | C(1)–C(5) | C(1)–C(2) | C(10)–N(21) | $\delta r$ | $\phi$ | $\theta$ |
|-----------------------|------------|-----------|-----------|-------------|------------|--------|----------|
| <b>3</b>              | 1.5096     | 1.4537    | 1.3778    | 1.3677      | 0.0375     | 108.4  | 156.4    |
| <b>3<sup>-</sup></b>  | 1.4241     | 1.4837    | 1.4274    | 1.3990      | 0.0193     | 151.5  | 133.3    |
| <b>3<sup>2-</sup></b> | 1.3849     | 1.4884    | 1.4787    | 1.4377      | 0.0132     | 154.0  | 140.6    |
| <b>8</b>              |            | 1.4366    | 1.3708    | 1.3675      | 0.0384     |        | 180.0    |
| <b>8<sup>-</sup></b>  |            | 1.4163    | 1.4284    | 1.4352      | 0.0355     |        | 179.7    |
| <b>9</b>              | 1.4326     |           | 1.3627    |             |            | 180.0  |          |
| <b>9<sup>-</sup></b>  | 1.3847     |           | 1.4149    |             |            | 180.0  |          |
| <b>9<sup>2-</sup></b> | 1.3518     |           | 1.4744    |             |            | 180.0  |          |

**TABLE 5: Energies of 3, 8, and 9 and Their Respective Anions (in kcal/mol)**

|                       | electron affinities <sup>a</sup> |                                | orbital interaction energies <sup>b</sup>      |  |  |  |   |  |
|-----------------------|----------------------------------|--------------------------------|--|--|--|--|---|--|
|                       | $E_{\text{ea}}^{\text{vert}}$    | $E_{\text{ea}}^{\text{adiab}}$ | $\pi_{\text{=}} \rightarrow \pi_{\text{CN}}^*$ | $\pi_{\text{CN}} \rightarrow \pi_{\text{=}}^*$ | $\pi_{\text{=}} \rightarrow \pi_{\text{Ph}}^*$ | $\pi_{\text{Ph}} \rightarrow \pi_{\text{=}}^*$ | $\pi_{\text{=}} \rightarrow \pi_{\text{=}}^*$ | $p_{\text{z,N}} \rightarrow \pi_{\text{Ph}}^*$ |
| <b>3</b>              | -39.44                           | -51.46                         | 39.05  | 16.53  | 8.03   | 22.45  | 0.87  | 50.71  |
| <b>3<sup>-</sup></b>  | 34.30                            | 25.26                          | 51.84 <sup>c</sup>                             | 12.69 <sup>c</sup>                             | 4.37 <sup>c</sup>                              | 10.36 <sup>c</sup>                             | 12.79 <sup>c</sup>                            | 38.18 <sup>c</sup>                             |
| <b>3<sup>2-</sup></b> |                                  |                                | 77.14 <sup>c</sup>                             | 6.20 <sup>c</sup>                              | 4.91 <sup>c</sup>                              | 13.25 <sup>c</sup>                             | 15.79 <sup>c</sup>                            | 17.99 <sup>c</sup>                             |
| <b>8</b>              | -21.49                           | -27.29                         | 42.21  | 15.55  | 9.36   | 27.75  |   | 51.22  |
| <b>8<sup>-</sup></b>  |                                  |                                | 51.89 <sup>c</sup>                             | 11.09 <sup>c</sup>                             | 14.94 <sup>c</sup>                             | 21.07 <sup>c</sup>                             |   | 10.05 <sup>c</sup>                             |
| <b>9</b>              | -71.38                           | -75.47                         | 34.04  | 19.77  |  |  | 16.28   |  |
| <b>9<sup>-</sup></b>  | 40.64                            | 36.21                          | 53.15 <sup>c</sup>                             | 12.95 <sup>c</sup>                             |  |  | 16.90 <sup>c</sup>                            |  |
| <b>9<sup>2-</sup></b> |                                  |                                | 77.49 <sup>c</sup>                             | 6.93 <sup>c</sup>                              |  |  | 17.96 <sup>c</sup>                            |  |

<sup>a</sup>  $E_{\text{ea}}^{\text{vert}}$  and  $E_{\text{ea}}^{\text{adiab}}$  stand for the vertical and adiabatic electron affinity. <sup>b</sup> The first two energies reflect the interaction of the  $\pi$  orbitals of both cyano groups with the neighboring vinyl group ( $\pi_{\text{CN}} \rightarrow \pi_{\text{=}}^*$ ) and vice versa ( $\pi_{\text{=}} \rightarrow \pi_{\text{CN}}^*$ ). The last column shows the donor interaction of the nitrogen lone pair with the phenyl ring ( $p_{\text{z,N}} \rightarrow \pi_{\text{Ph}}^*$ ). All other interaction energies are described in Table 2. <sup>c</sup> For comparison, the values of the ionic compounds are computed with the Lewis structure optimal for their neutral state.

**Figure 4.** Optimal Lewis structures of **3** (neutral and twofold charged anion) with the dominant conjugation paths.

the first reduction potential of **3** (and also of the fragment molecules **8** and **9**) is negative, while in the gas phase the second electron of **3<sup>2-</sup>** and **9<sup>2-</sup>** is not bound. The difference between the vertical and the adiabatic electron affinities is indicative of a large relaxation in both reduction steps of **3**, in contrast to the only small difference for the planar anions of **9**. Structural rearrangements in the reduction process of **3** were anticipated already by Diederich and co-workers based on the examination of the oxidation wave shape.<sup>5</sup>

Inspection of the geometry of **3** and its anions (Table 4) indeed reveals large changes in bond lengths and torsion angles. While the backbone of **3** takes a structure similar to **1c**, **3<sup>-</sup>** and **3<sup>2-</sup>** resemble the structure of **1b** with substantial butadiene conjugation. The shortening of the C(1)–C(11) bond by as much as 0.12 Å from **3** to **3<sup>2-</sup>** suggests the formation of a double bond between these two atoms. The optimal Lewis structure therefore is different from the one of the neutral compound (Figure 4). The  $\pi$  system of **3**, which is divided into two vastly noninteracting styrene units (Figure 4a), is changed upon reduction forming two geminally linked acceptor–acceptor paths and an extended through-conjugation path that connects both phenyl rings via the newly formed double bond (Figure 4b).

The orbital occupations listed in Table 6 show that most of the additional charge of the anions is located at C(2)/C(12) as well as on the adjacent cyano groups. A minor amount of additional charge is found on the dimethylamino groups, where

**TABLE 6: Occupation of the  $\pi$  System in 3, 8, and 9 and Their Respective Anions<sup>a</sup>**

|                       | CN    | C(2)  | C(1)  | phenyl | NMe <sub>2</sub> | total  | formal |
|-----------------------|-------|-------|-------|--------|------------------|--------|--------|
| <b>3</b>              | 4.094 | 1.167 | 0.915 | 6.063  | 1.677            | 13.916 | 14.0   |
| <b>3<sup>-</sup></b>  | 4.220 | 1.261 | 1.015 | 6.108  | 1.743            | 14.347 | 14.5   |
| <b>3<sup>2-</sup></b> | 4.378 | 1.418 | 1.064 | 6.091  | 1.781            | 14.731 | 15.0   |
| <b>8</b>              | 4.110 | 1.190 | 0.881 | 6.062  | 1.677            | 13.918 | 14.0   |
| <b>8<sup>-</sup></b>  | 4.329 | 1.313 | 1.087 | 6.282  | 1.837            | 14.847 | 15.0   |
| <b>9</b>              | 4.005 | 1.072 | 0.907 |        |                  | 5.984  | 6.0    |
| <b>9<sup>-</sup></b>  | 4.220 | 1.250 | 1.008 |        |                  | 6.478  | 6.5    |
| <b>9<sup>2-</sup></b> | 4.468 | 1.406 | 1.100 |        |                  | 6.974  | 7.0    |

<sup>a</sup> The occupation numbers of the following  $p_z$  orbitals are listed: the cyano groups attached to C(3) and C(4), the carbon atoms C(1) and C(2) of the vinylic bond, as well as the phenyl group C(5)–C(10) and the lone pair of N(21), further the total occupation in one half of the  $\pi$  system and the formal (integer) occupation number expected from the Lewis structure.

the nitrogen atom adopts an  $sp^3$  hybridization, with the group thereby losing most of its donor capability as indicated by the decay of the orbital interaction energy from the nitrogen  $p_z$  to the phenyl ring upon reduction (Table 5). This same observation is also made for **8<sup>-</sup>**. The low quinoid character of the anions of **3** and the much longer C(10)–N(21)/C(20)–N(22) bonds show that no significant D–A interaction is present anymore in **3<sup>-</sup>** and **3<sup>2-</sup>**.

Both anions of **3** now also show significant orbital interactions along the butadiene path (which were almost completely absent

in the neutral compound). In return, the phenyl–vinyl interactions decrease to one-half. The comparison with tetracyanobutadiene **9** shows that both anions take a similar molecular structure. The charge donation to the cyano groups is strongly increased, establishing two new identical geminal conjugation paths. Geminal acceptor–acceptor paths with unexpectedly high delocalization energies have been found in other donor-substituted cyanoethynylethenes.<sup>17</sup>

The Lewis structure presented in Figure 4b therefore offers an adequate representation of the electronic structure of the anions. The interaction energies along the butadiene bridge for **3**<sup>2-</sup> and **9**<sup>2-</sup> are very similar, regardless of the underlying Lewis structure. The interaction between the cyano groups and the double bond (or the lone pair in Lewis structure **3b**) is more pronounced in **9**<sup>2-</sup>, which contrary to **3**<sup>2-</sup> is fully planar. Accordingly, the orbital occupation numbers for the cyano groups in **3**<sup>2-</sup> are smaller than those in **9**<sup>2-</sup>.

In contrast to the neutral compound **3**, which is best described as an  $\alpha,\alpha$ -coupled bistyryl, the anions of **3** take a molecular and electronic structure which represents a switch back to a substituted butadiene structure. We would expect that the same result can be achieved by means of optical excitation.

## Conclusions

2,3-Diphenylbutadiene (**1**) and its D–A substituted derivatives **2** and **3** are branched  $\pi$  systems that are nonplanar due to steric strain. The details of their molecular structure is governed by electron delocalization along the butadiene- and styrene-type conjugation paths. Conjugation along these two paths can be switched on and off by rotation about the single bonds C(1)–C(11) and C(1)–C(5) measured by the angles  $\phi$  and  $\theta$ .

The unsubstituted **1** as well as the D–A substituted diphenylbutadiene **2** show two minima that differ in energy by less than 1 kcal/mol. The corresponding structures **a** and **b** represent a compromise with one dominant conjugation path. This can nicely be illustrated by means of the NBO analysis. The saddle points **c** and **d**, on the other hand, represent structures with one of the two conjugation paths switched on, and the other one switched off. The PES of **1** shows that there are low-energy saddle points that connect the minimum energy structures (and their mirror images) via a low-energy path. This indicates, that both minima could be populated by external stimuli.

In **2** there are only weak D–A interactions across the doubly bifurcated cross-conjugation path connecting the two functional groups. They are not strong enough to overturn the equilibrium structure of **2**.

**3**, with its two through-conjugated D–A paths, shows a vastly different picture: there is only one minimum on the PES, which is best described as an  $\alpha,\alpha$ -coupled bistyryl. Apparently, the loss of conjugation in the butadiene backbone is marginal compared to the gain in D–A conjugation along the styrene system. The view of **3** as two nearly independent D–A substituted styrene units also explains its cyclic voltametry spectrum reported by Diederich.

Most interestingly though, the anions of **3** take a strongly different molecular and electronic structure. The negative charge is essentially located on the butadiene backbone leading to one

through-conjugated donor–donor path and two cross-conjugated acceptor–acceptor paths. As a consequence, the molecular structure undergoes much geometrical change. This explains the potential of **3** as a very interesting compound also for electrochemical and photochemical applications.

**Acknowledgment.** This work was supported by the Swiss National Science Foundation through Grant 200021-108066. The authors acknowledge a generous allocation of computer time granted by C<sup>4</sup> as well as fruitful discussions with Prof. C. A. van Walree.

## References and Notes

- (1) Lutz, M.; Spek, A. L.; van der Wiel, B. C.; van Walree, C. A. *Acta Cryst.* **2005**, *C61*, o300.
- (2) van Walree, C. A.; van der Wiel, B. C.; Jennekens, L. W.; Lutz, M.; Spek, A. L.; Havenith, R. W. A.; van Lenthe, J. H. *Eur. J. Org. Chem.* **2007**, *28*, 4746.
- (3) van der Wiel, B. C.; Williams, R. M.; van Walree, C. A. *Org. Biomol. Chem.* **2004**, *2*, 3432.
- (4) Michinobu, T.; May, J. C.; Lim, J. H.; Boudon, C.; Gisselbrecht, J.-P.; Seiler, P.; Gross, M.; Biaggio, I.; Diederich, F. *Chem. Commun.* **2005**, *6*, 737.
- (5) Michinobu, T.; Boudon, C.; Gisselbrecht, J. P.; Seiler, P.; Frank, B.; Moonen, N. N. P.; Gross, M.; Diederich, F. *Chem. Eur. J.* **2006**, *12*, 1889.
- (6) Fernández, I.; Frenking, G. *Chem. Eur. J.* **2006**, *12*, 3617.
- (7) Schleyer, P. v. R.; Maerker, C.; Dransfeld, A.; Jiao, H.; Hommes, N. J. R. v. E. *J. Am. Chem. Soc.* **1996**, *118*, 6317.
- (8) Fernández, I.; Frenking, G. *J. Org. Chem.* **2006**, *71*, 2251.
- (9) Heine, T.; Schleyer, P. v. R.; Corminboeuf, C.; Seifert, G.; Reviakine, R.; Weber, J. *J. Phys. Chem. A* **2003**, *107*, 6470.
- (10) Zhao, Y.; Zhou, N.; Slepokov, A. D.; Ciulei, S. C.; McDonald, R.; Hegmann, F. A.; Tykwinski, R. R. *Helv. Chim. Acta* **2007**, *90*, 909.
- (11) (a) Brunck, T. K.; Weinhold, F. *J. Am. Chem. Soc.* **1979**, *101*, 1700. (b) Foster, J. P.; Weinhold, F. *J. Am. Chem. Soc.* **1980**, *102*, 7211. (c) Reed, A. E.; Weinstock, R. B.; Weinhold, F. *J. Chem. Phys.* **1985**, *83*, 735. (d) Reed, A. E.; Weinhold, F. *J. Chem. Phys.* **1985**, *83*, 1736. (e) Reed, A. E.; Curtiss, L. A.; Weinhold, F. *Chem. Rev.* **1988**, *88*, 899.
- (12) Bruschi, M.; Giuffreda, M. G.; Lüthi, H. P. *Chem. Eur. J.* **2002**, *8*, 4216.
- (13) Giuffreda, M. G.; Bruschi, M.; Lüthi, H. P. *Chem. Eur. J.* **2004**, *10*, 5617.
- (14) Bruschi, M.; Giuffreda, M. G.; Lüthi, H. P. *Chimia* **2005**, *59*, 539.
- (15) Frisch, M. J.; Trucks, G. W.; Schlegel, H. B.; Scuseria, G. E.; Robb, M. A.; Cheeseman, J. R.; Montgomery, J. A., Jr.; Vreven, T.; Kudin, K. N.; Burant, J. C.; Millam, J. M.; Iyengar, S. S.; Tomasi, J.; Barone, V.; Mennucci, B.; Cossi, M.; Scalmani, G.; Rega, N.; Petersson, G. A.; Nakatsuji, H.; Hada, M.; Ehara, M.; Toyota, K.; Fukuda, R.; Hasegawa, J.; Ishida, M.; Nakajima, T.; Honda, Y.; Kitao, O.; Nakai, H.; Klene, M.; Li, X.; Knox, J. E.; Hratchian, H. P.; Cross, J. B.; Bakken, V.; Adamo, C.; Jaramillo, J.; Gomperts, R.; Stratmann, R. E.; Yazyev, O.; Austin, A. J.; Cammi, R.; Pomelli, C.; Ochterski, J. W.; Ayala, P. Y.; Morokuma, K.; Voth, G. A.; Salvador, P.; Dannenberg, J. J.; Zakrzewski, V. G.; Dapprich, S.; Daniels, A. D.; Strain, M. C.; Farkas, O.; Malick, D. K.; Rabuck, A. D.; Raghavachari, K.; Foresman, J. B.; Ortiz, J. V.; Cui, Q.; Baboul, A. G.; Clifford, S.; Cioslowski, J.; Stefanov, B. B.; Liu, G.; Liashenko, A.; Piskorz, P.; Komaromi, I.; Martin, R. L.; Fox, D. J.; Keith, T.; Al-Laham, M. A.; Peng, C. Y.; Nanayakkara, A.; Challacombe, M.; Gill, P. M. W.; Johnson, B.; Chen, W.; Wong, M. W.; Gonzalez, C.; Pople, J. A. *Gaussian 03*, revision D.01; Gaussian, Inc.: Wallingford, CT, 2004.
- (16) Sinnokrot, M. O.; Sherrill, C. D. *J. Phys. Chem. A* **2006**, *110*, 10656.
- (17) Giuffreda, M. G.; Lüthi, H. P.; Moonen, N. N. P.; Diederich, F. *Chem. Eur. J.* to be submitted.
- (18) (a) Dehu, C.; Meyers, F.; Brédas, J. L. *J. Am. Chem. Soc.* **1993**, *115*, 6198. (b) Hilger, A.; Gisselbrecht, J.-P.; Tykwinski, R. R.; Boudon, C.; Schreiber, M.; Martin, R. E.; Lüthi, H. P.; Gross, M.; Diederich, F. *J. Am. Chem. Soc.* **1997**, *119*, 2069.